Ultra-sensitive SiGe Bipolar Phototransistors for Optical Interconnects

Michael Roe

Electrical Engineering and Computer Sciences
University of California at Berkeley

Technical Report No. UCB/EECS-2012-123
http://www.eecs.berkeley.edu/Pubs/TechRpts/2012/EECS-2012-123.html

May 27, 2012

Ultra-Sensitive SiGe Bipolar Phototransistors for Optical Interconnects

by Michael Roe

Research Project

Submitted to the Department of Electrical Engineering and Computer Sciences, University of California at Berkeley, in partial satisfaction of the requirements for the degree of **Master of Science, Plan II**.

Approval for the Report and Comprehensive Examination:

Committee:

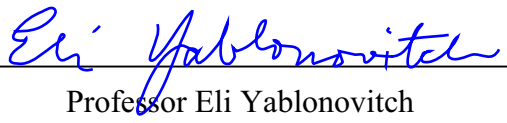

Professor Eli Yablonovitch
Research Advisor

5/10/2012

(Date)

* * * * * * *

Professor Ming Wu
Second Reader

5/9/2012

(Date)

Table of Contents

1. Introduction

Traditional electrical wiring has become limited in terms of bandwidth capacity and power consumption. As digital circuit elements have reduced in size and increased in speed, electrical interconnects have been struggling to keep up with the bandwidth demands [1]. The primary factors holding back copper wires are high capacitance and inherent dielectric losses. The industry has compensated by placing repeaters and amplifiers along electrical links [2]. However, these methods increase circuit complexity and energy consumption.

As a result, optical interconnects have been proposed to replace traditional electrical wiring [3]. Candidate receivers for these systems include high-speed photodiodes [4], high-sensitivity avalanche photo-diodes (APDs) [5], and phototransistors [6]. While photodiodes themselves do not consume a large amount of energy, the device is often followed by stages of amplifiers in order to achieve the required system sensitivity. The chain of trans-impedance amplifiers consumes the majority of the power in this photo-detector system [7]. Similarly, although APDs can achieve high receiver sensitivity for a small number of photons, avalanche diodes require a large reverse bias voltage for impact ionization [3].

On the other hand, phototransistors offer an alternative for low-power optical detection. Others have proposed optical field-effect transistors (FETs) including photo-heterojunction JFETs (photo-hetero-JFETs) [8] and CMOS devices [9]. We will focus on the photo-bipolar junction transistor (photo-BJT) and heterojunction phototransistor (HPT) because of the large current gain of such devices. In Figure 1, the photo-BJT system is compared to the PD receiver system in terms of power consumption and complexity.

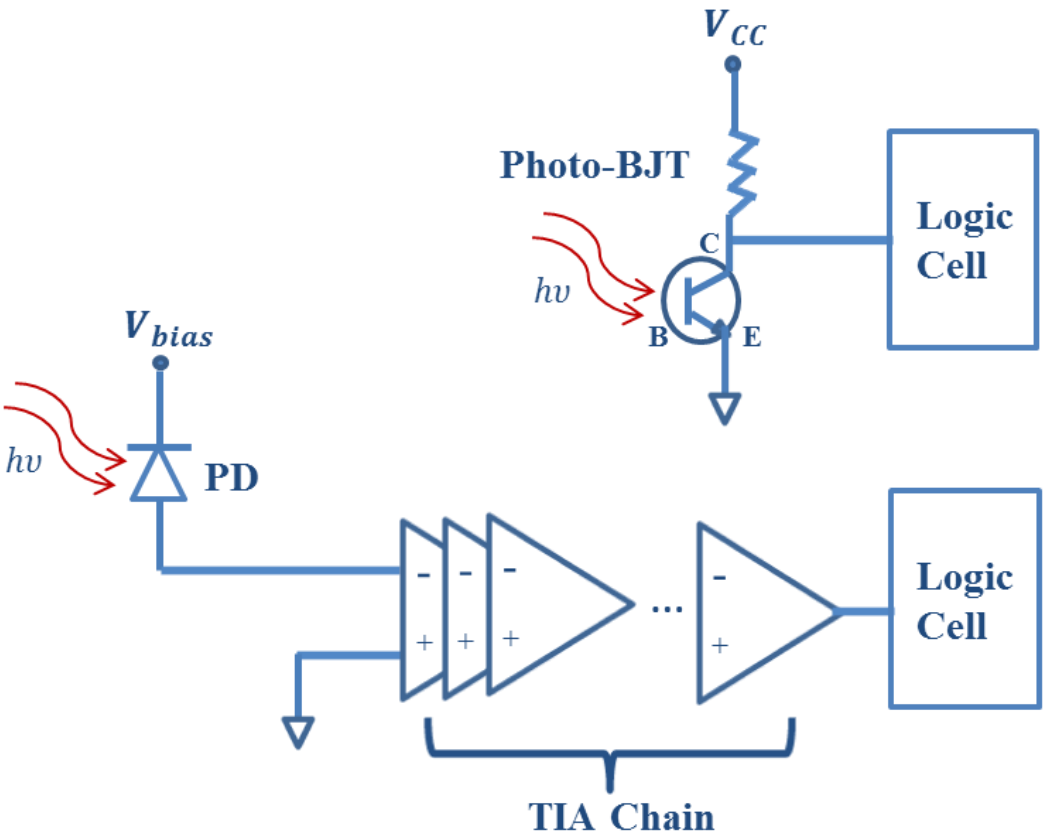

Figure 1: The advantage of the photo-BJT receiver scheme (top) is that it does not require the power-hungry chain of trans-impedance amplifiers (TIAs) that the photo-detector (PD) receiver scheme (bottom) uses. Instead, the light shone on the base is amplified by the inherent transistor action of the BJT, resulting in a reduced number of photons per bit than the PD. This reduces system complexity, cost, and power consumption.

The photo-bipolar transistor is not a novel idea. In fact, it was proposed by Shockley in 1951 [10]. The bipolar phototransistor was first fabricated using germanium [11] and then extended to heterojunction structures by Kroemer [12]. These devices were once thought to be too complex and costly to produce. However, due to trends in device scaling and improvements in fabrication technology, the photo bipolar transistor is a promising candidate for modern optical receivers systems. In this paper, we will limit our discussion to the gain mechanisms of germanium photo-BJTs and Si-Ge HPTs for ultra-sensitive light detection. We focus on germanium devices because they can be easily integrated with industry-standard CMOS and BiCMOS processes.

2. Homojunction Bipolar Phototransistors

In this section, we derive the gain mechanism of the photo-BJT. Then, we analyze the band structure and physics of a Si-Ge bipolar phototransistor. Finally, we estimate the current voltage characteristics of a Si-Ge photo-BJT.

2.1 Photo-BJT Gain Model

We begin by considering a typical npn BJT of width w and cross-sectional area ld and emitter, base, and collector contacts. The key difference between this and the photo-BJT is a floating base. The voltage bias on the base is supplied by shining constant or pulsed light, instead of by an electrode. That is, part of the base current is given by light-induced electron-hole pairs.

For a photo-BJT in active mode, the emitter-base junction (EBJ) is forward-biased and the collector-base junction (CBJ) is reverse-biased. Refer to the photo-BJT band diagram shown in Figure 2. For a constant light source, the photo-voltage supplied to the EBJ is:

$$V_{BE,ph} = \Delta V = \frac{Q_p}{C_{EBJ}} = \frac{q\delta p}{C_{EBJ}} lwd \tag{2.1}$$

In this equation, C_{EBJ} is the capacitance of the EBJ and δp is the photo-induced hole concentration. In forward active mode, the photo-generated electrons are swept to the reverse-biased collector region ($\delta n \to 0$). Given a constant light source of power P_{opt} and energy $h\upsilon$ allows us to simplify (2.1):

$$V_{BE,ph} = \Delta V = \frac{q\delta p}{C_{EBJ}} lwd = \frac{qG_0\tau_p}{C_{EBJ}} lwd = \eta \frac{qP_{opt}\tau_p}{h\upsilon C_{EBJ}} \tag{2.2}$$

For details of the simplification in the last line, see Appendix B: Photoconductors. In equation (2.2), G_0 is the generation rate, τ_p is the base recombination rate, and η is the total base quantum efficiency. Now, we use the capacitance of a standard PN junction:

$$C_{EBJ} = A\sqrt{\frac{q\varepsilon}{2\Delta V}\frac{N_D N_A}{N_D + N_A}} \tag{2.3}$$

where ε is the material permittivity, A is the cross sectional area, N_D is emitter doping concentration, and N_A is the base doping concentration. Combining (2.2) and (2.3), we obtain an expression for the photo-induced base voltage:

$$V_{BE,ph} = \Delta V = \frac{2q}{\varepsilon}\left(\eta \frac{P_{opt}\tau_p}{A\,h\upsilon}\right)^2 \left(\frac{N_D+N_A}{N_D N_A}\right) \tag{2.4}$$

Recall that the gain parameter of a BJT can be maximized for $N_A \ll N_D$ (lightly doped base). In this case:

$$V_{BE,ph} \approx \frac{2q}{\varepsilon N_A}\left(\eta \frac{P_{opt}\tau_p}{A\,h\upsilon}\right)^2 \tag{2.5}$$

This photo-voltage can be plugged into the gain equation for a BJT to obtain the current response for a photo-BJT. The collector current i_C is:

$$i_C = \beta i_B = \beta I_s\, e^{v_{BE,ph}/V_T} \tag{2.6}$$

where the gain parameter β is the same as for a typical bipolar transistor:

$$\beta = \frac{1}{\frac{W^2}{2D_n\tau_n} + \frac{W D_p N_A}{L_p D_n N_D}} \tag{2.7}$$

For details, see Appendix A: Homojunction BJT Physics.

Therefore, the most important difference between the gain mechanism of the standard BJT and the floating base photo-BJT is the exponential dependence on a photo-voltage $V_{BE,ph}$. instead of an electrical voltage. Based on equations (2.5-2.7), we have the following photo-BJT design considerations:

(1) The collector current depends exponentially on:
    a. the optical input power.
    b. the recombination lifetime in the base.
    c. the quantum efficiency of the base.
(2) The same first-order design rules of a homojunction BJT still apply:
    a. Minimize the base width, which is approximately quadratic with the gain parameter.

b. Minimize N_A/N_D (lightly doped base and heavily doped emitter), which is inversely proportional to the gain parameter. For a photo-BJT, having a lightly-doped base also exponentially increases the photo-voltage.

In the following section, we will make extensive use of these rules when analyzing a Ge photo-BJT.

2.2 Band Diagram and Analysis

Now we turn our attention to the band diagram and physical description of the gain mechanism of the photo-BJT. Refer to Figure 2 below for the equilibrium and forward active band diagrams of a Ge photo-BJT.

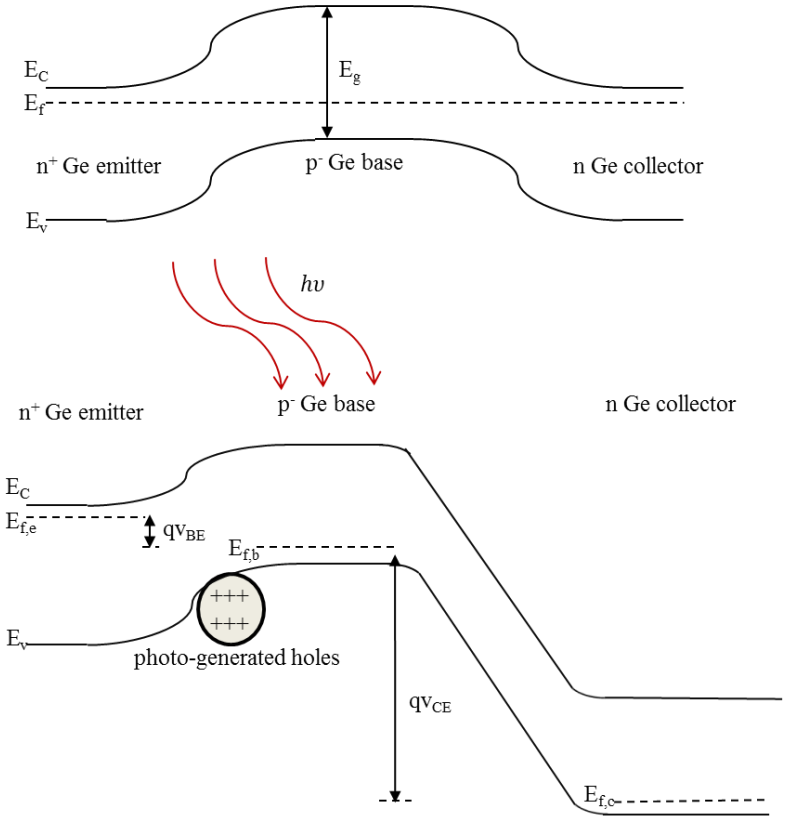

Figure 2: Band diagram for Ge photo-BJT in equilibrium (top) and in forward active mode (bottom). In forward active mode, the emitter-base junction (EBJ) if forward biased by shining light on the floating base. The collector-base junction (CBJ) is reverse biased. Therefore, the large voltage drop across the CBJ collects electrons that diffuse across the base region. The EBJ and CBJ voltages create quasi-fermi levels in the three regions.

In equilibrium, the minority carrier electrons in the quasi-neutral region are unable to overcome the barrier created by the p-type base. In forward active mode, we reverse bias the CBJ and forward bias the EBJ by shining light on the base junction. Photo-generated electrons are swept across the base region to the collector contact because of the reverse biased CBJ. However, in the valence band, photo-generated holes do not have enough energy to overcome the barrier created by the emitter-base PN junction. These photo-generated holes build up and create a positive base-emitter voltage, thereby reducing the conduction band barrier. This allows the conduction band electrons to surmount the EBJ energy barrier. As long as the electron diffusion length is larger than the base width, these electrons are able to diffuse across the base and reach the reverse biased collector region. Thus, we lightly dope the base relative to the emitter to improve the electron injection efficiency into the base and the gain of the device.

For a photo-BJ, it is especially important to make the emitter to base doping ratio as large as possible, not only to increase the gain of the device but also to increase the carrier generation near the EBJ. That is, in the quasi-neutral region of the EBJ most of the depletion width will be in the lightly doped base creating a larger absorption region. In forward active mode, this will result in a higher base responsivity so that most of the EHPs generated within one diffusion length from the base will be immediately swept to the collector region.

The other design rule stated in section 2.1 was to make the base width short relative to the diffusion length. The gain parameter is very sensitive to base width. If the minority carrier electrons are able to diffuse across the base without recombining with holes, the photoconductive gain of the system will be large. This concept is illustrated in Figure 3 for various emitter to base doping ratios.

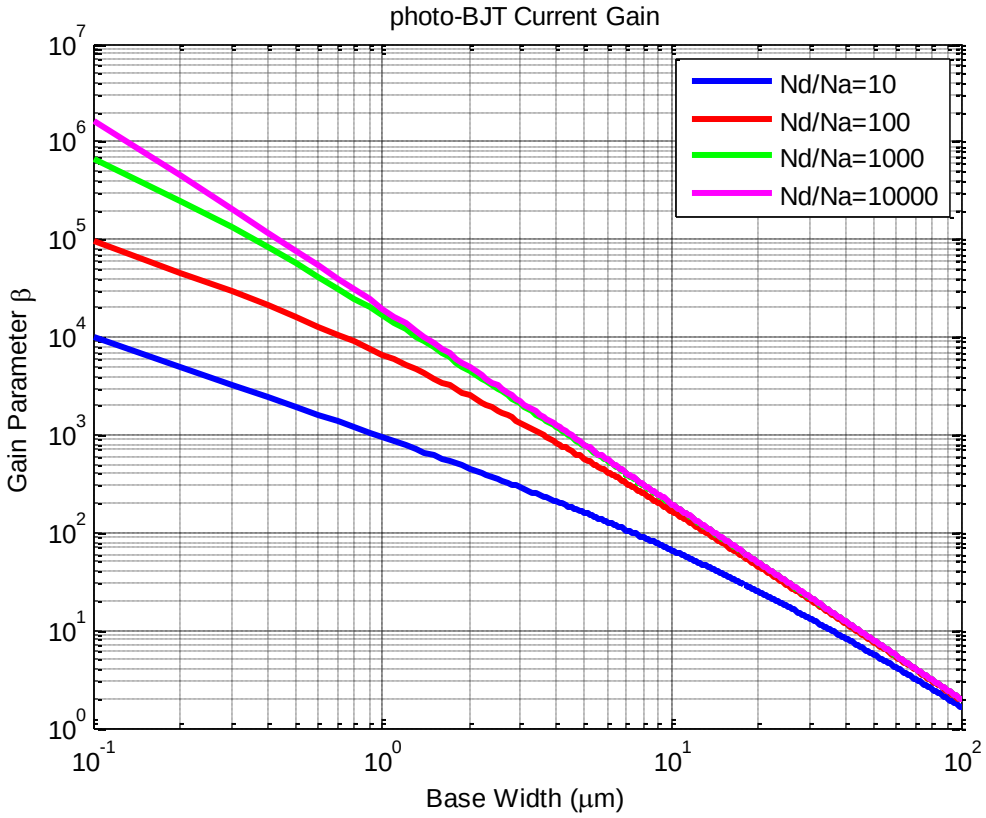

Figure 3: Plot of gain parameter for photo-BJT as a function of base width for different emitter to base doping ratios N_d/N_a and conservative diffusion lengths $L_p = L_n = 100\mu m$. This plot indicates that a good first order design would implement are narrow base width and high emitter to base doping ratio.

The most important reason to implement a photo-BJT as an ultra-sensitive detector is that the collect current is an exponential function of the base-emitter photo-voltage. Figure 4 shows the I-V curve of the photo-BJT. The system photo-voltage is dependent to the number of incoming photons and the quantum efficiency of the base material. Thus, it is of utmost importance that the base region be made of high quality material to optimize the quantum efficiency and diffusion length and gain parameter. The large absorption coefficient of germanium makes it an ideal base material for detection of weak optical links. Given a bit-error-rate requirement, this calculation can be used to solve for a desired signal-to-noise ratio (SNR). From this required SNR, we can obtain the number of photons and photons per bit to operate the photo-BJT in a detector system.

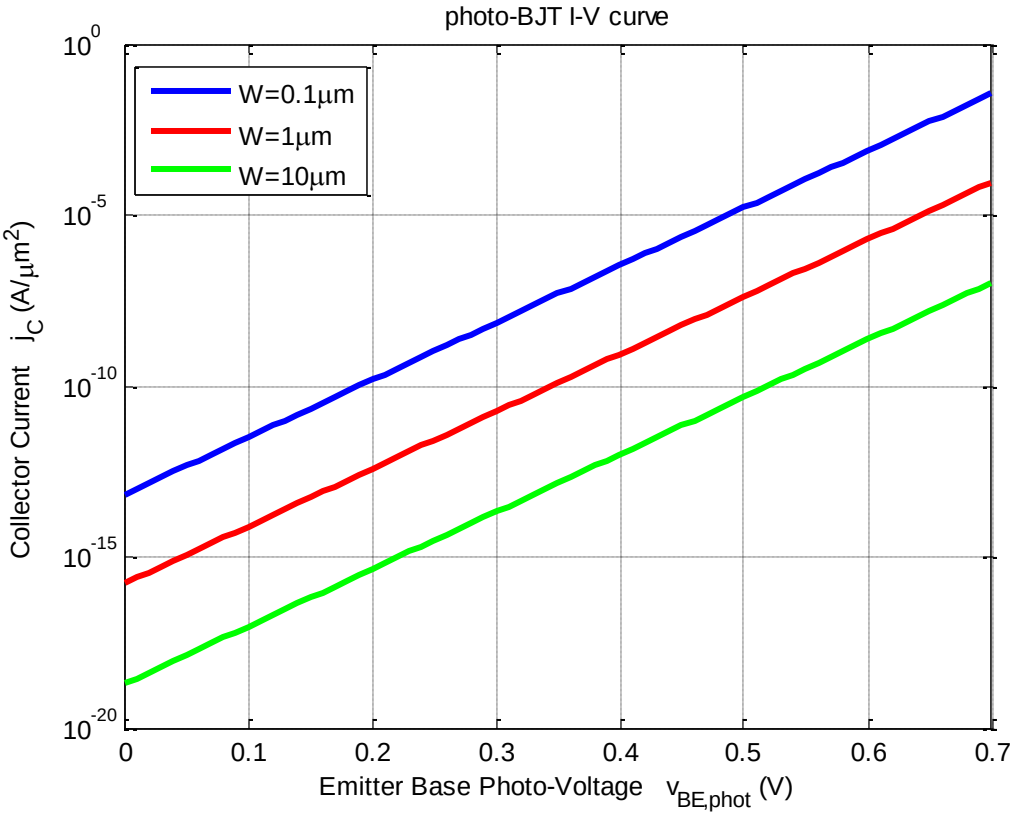

Figure 4: First order plot of collector current vs. EBJ photo-voltage for the photo-BJT. We assume a conservative diffusion length $L_p = L_n = 100\mu m$ and emitter to base doping ratio of 1000. The collector current is extremely sensitive to photo-voltage and the number of photons incident on the base. The current gain of the system also varies by orders of magnitude with decreased base width. It is important to note that this plot does not consider system non-idealities, such as velocity saturation and the Kirk effect, both of which will be sensitive to base width scaling.

3. Heterojunction Bipolar Phototransistors

The band structure of heterojunction bipolar phototransistors (HPTs) allow them achieve current gains that are much larger than photo-BJTs. In the follow section we will generalize the gain mechanism of HPTs and then analyze the case of SiGe HPT for use in a monolithic optical interconnect system.

3.1 Comparison of HPT and photo-BJT Gain Models

In this section, we compare the gain performance of the HPT and photo-BJT. Refer to the HPT band diagram shown in Figure 5. We consider a single heterojunction between the emitter and base so that the collector and base are made of the same material.

Again, the key difference between the heterojunction bipolar transistor (HBT) and HPT is a floating base that is illuminated. The incident photons generate EHPs in the base creating a photo-voltage given by equation (2.5). For heterojunction materials with similar permittivities, we can assume that the emitter base capacitance and therefore the photo-voltage is similar to that of a photo-BJT. Just as for a photo-BJT, the HPT is exponential with this photo-voltage.

The current gain of the HPT is different from the photo-BJT. Recall that the gain parameter β can be written in terms of two key parameters, the base transport factor:

$$\alpha_T = 1 - \frac{W^2}{2L_n^2} \tag{3.1}$$

and the emitter injection efficiency:

$$\gamma_{hetero} = \left(1 + \frac{D_p L_n N_{a,b}}{D_n L_p N_{d,e}} \exp\left(-\frac{\Delta E_g}{kT}\right)\right)^{-1} \tag{3.2}$$

$$\gamma_{homo} = \left(1 + \frac{D_p L_n N_{a,b}}{D_n L_p N_{d,e}}\right)^{-1} \tag{3.3}$$

where W is the base width and L_n is the electron diffusion length in the base. For details see Appendix C: Heterojunction BJT Physics.

Now, for either type of bipolar transistor, the gain parameter can be written as:

$$\beta = \frac{\gamma \alpha_T}{1-\gamma \alpha_T} \sim \frac{1}{1-\gamma \alpha_T} \tag{3.4}$$

In the last line, I have made the approximation that the efficiency product is near unity, which is typical of a high performance bipolar transistor. Using equations (3.1)-(3.3), we can derive an expression for the ratio of gain parameters for an HBT and BJT.

$$\frac{\beta_{hetero}}{\beta_{homo}} \sim \left(\frac{L_{n,hetero}}{Ln,homo}\right)^2 \exp\left(\frac{\Delta E_g}{kT}\right) \tag{3.5}$$

When compared to the photo-BJT, the current gain performance of an HPT has the following tradeoff:

(1) For an HPT, the emitter to base current increases exponentially with the bandgap difference.
(2) However, heterojunction interfaces may contain defects, which shorten the diffusion length L_n relative to the base width. This quadratically decreases the base transport factor, thereby decreasing the gain.

We will explore this tradeoff further in the next section in terms of $Si_{1-x}Ge_x$ HPTs.

3.2 HPT Band Diagram and Analysis

Before we quantitatively analyze SiGe HPTs, we begin by giving a physical description of HPT gain. The forward active mode band diagram of a SiGe HPT is shown in Figure 5. The key to the higher current gain of the heterojunction bipolar transistor (HBT) is the bandgap narrowing and apparent heavy doping effect in the base. However, for an HPT, there is the added benefit of the conduction band offset in trapping photo-generated holes. Recall from the photo-BJT that these photo-generated holes reduce the EBJ barrier giving rise to the bipolar transistor gain. Furthermore, the discontinuity in the conduction band increases the lifetime of the photo-generated holes, thereby increasing the secondary photoconductivity of the HPT.

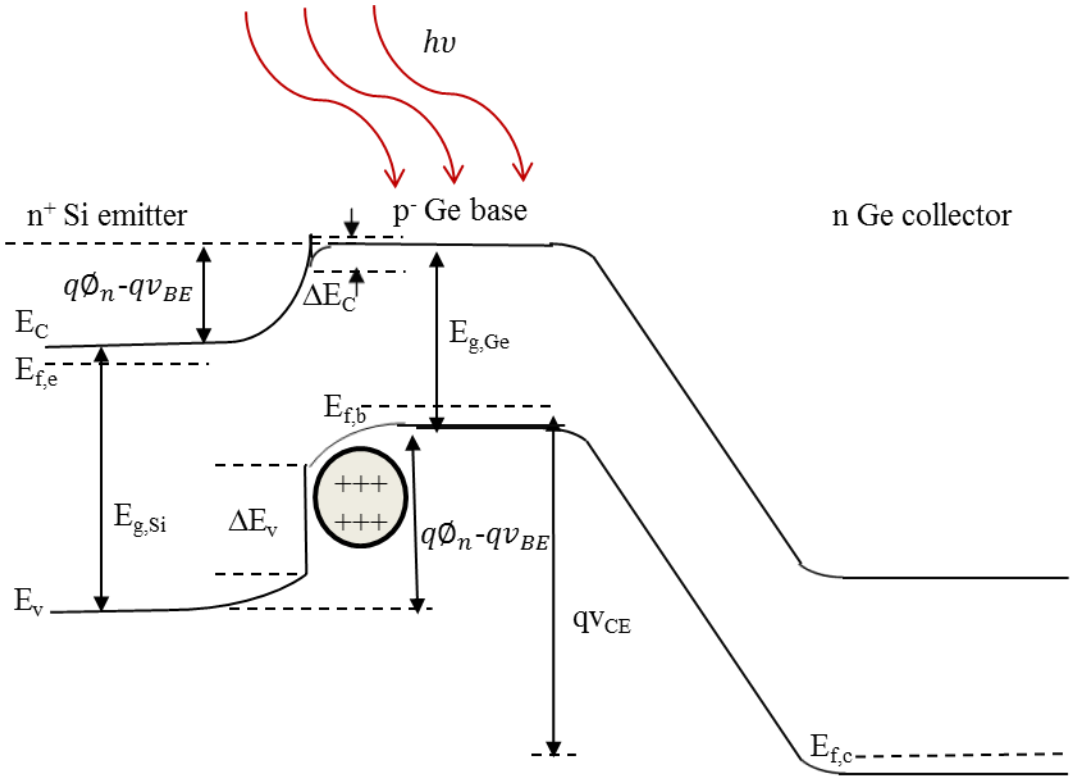

Figure 5: Band diagram of a SiGe bipolar npn HPT. The conduction band offset for the SiGe heterostructure is smaller than the valence band offset. This valence band offset helps to trap photo-generated holes near the EBJ contributing to a larger current gain. Another parameter improving the current gain of the HPT is the reduced bandgap in the base. The conduction band energy of the base is reduced by a factor of $q\phi_n$, which is exponential with the bandgap difference. This factor improves the emitter injection efficiency as more electrons are able to surmount the EBJ barrier.

Due to growth defects and the 4% lattice mismatch between Si and Ge, we must also consider the variation in diffusion lengths at the emitter base heterojunction interface. Even with the advances in SiGe growth processes, the diffusion length across the base will be shorter for an HPT than for a photo-BJT. The physics of this tradeoff is given by equation (3.5). Figure 6 shows this tradeoff for varying Ge concentrations, assuming (incorrectly) that the bandgap is a linear function of Ge content. While the quality of the interface reduces the gain coefficient of the HPT, it is still larger than the homojunction photo-BJT because of the exponential dependence on bandgap difference.

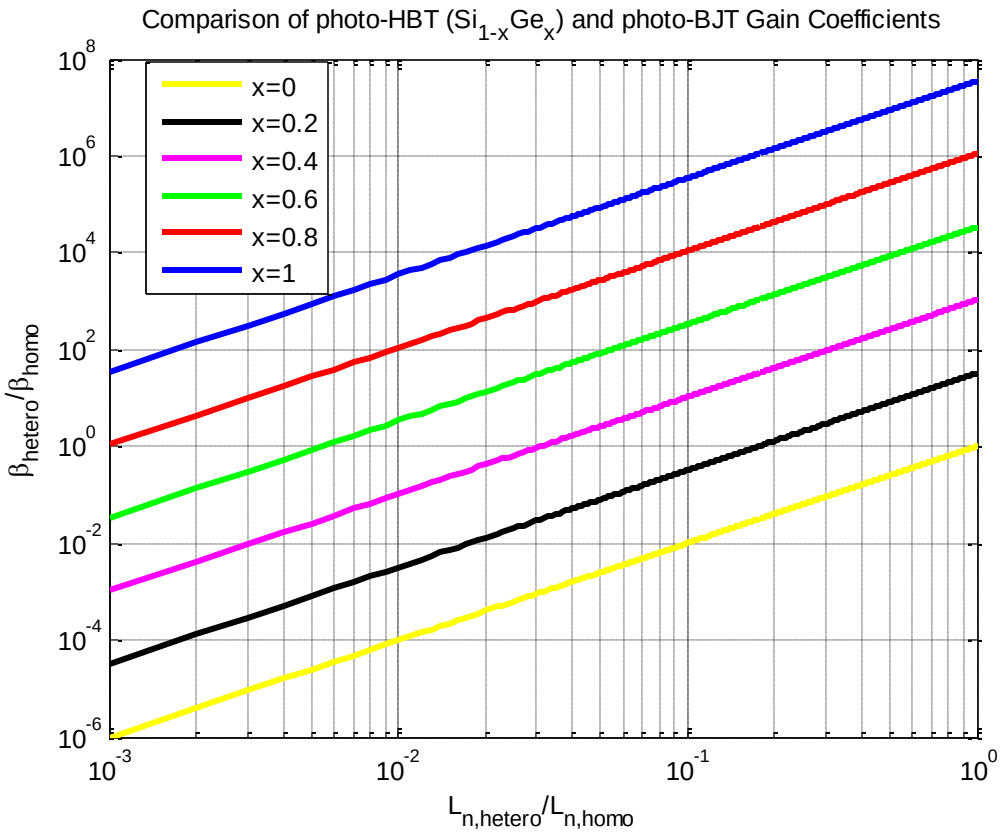

Figure 6: Plot of the tradeoff between bandgap difference and base diffusion length for the homojunction photo-BJT and the HPT. Even for an HBT with shorter base diffusion length than a BJT, the exponential bandgap difference still results in a larger gain coefficient. The plot is varied over Ge concentration in the quasi-neutral region between the emitter base junction (EBJ). The circuit designer can tailor the gain coefficient of a HPT by varying the Ge content in this graded junction.

Refer to Figure 7 for an estimate of the current densities that can be achieved for a SiGe HPT. This figure shows that the collector current for an HPT can be orders of magnitude larger than for a photo-BJT due to the bandgap difference for SiGe. Note that this plot does not include the change in photo-voltage with hole lifetime at the emitter base heterojunction. This change in hole lifetime is governed by two opposing factors: the interface defects of the heterojunction and the valence band discontinuity. Because the material lifetime is often determined experimentally, we will ignore the change in HPT hole lifetime for now. Even so, because of heterojunction physics and the exponential dependence on the photo-voltage, we have shown that the HPT is tailored for detecting and amplifying weak optical signals.

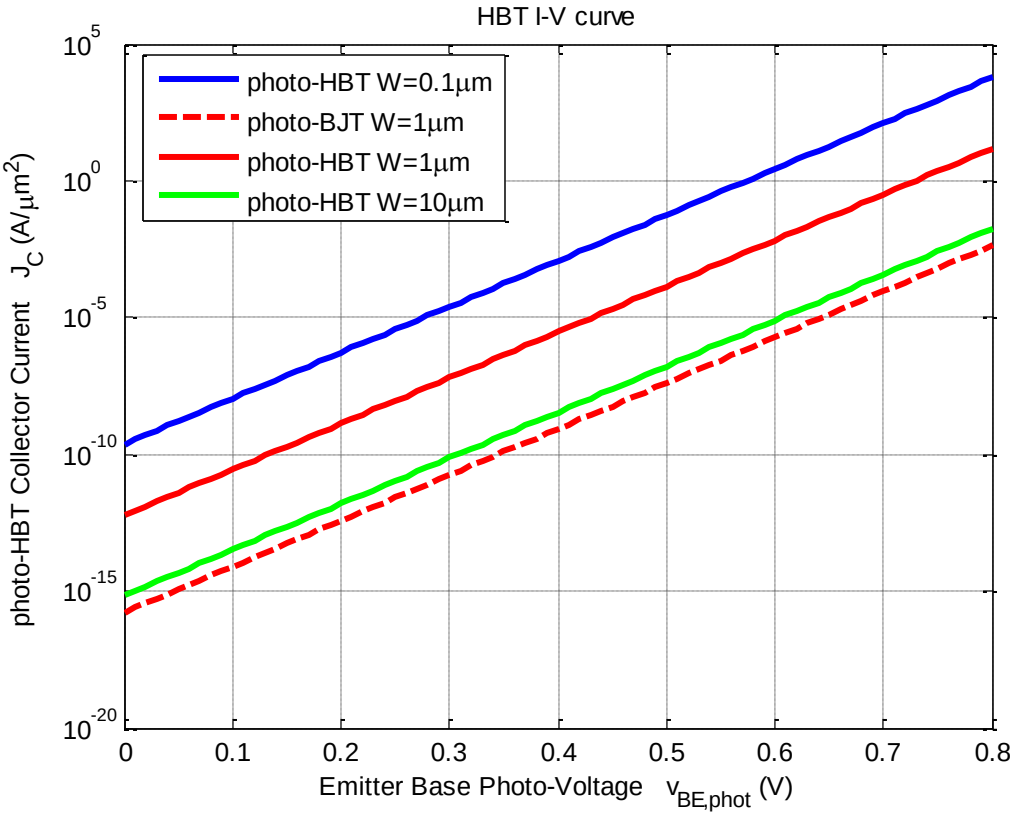

Figure 7: I-V curve of a SiGe npn HPT varied across base width and plotted against a Ge photo-BJT. Due to interface defects, we conservatively assume that the base diffusion length of the heterojunction is 100 times worse than that of a homojunction. Even so, the bandgap difference and increased density of states in the base improve the current and photo-responsivity of the HPT relative to the photo-BJT.

Conclusions

The smaller bandgap and large absorption coefficient of germanium at telecommunication wavelengths make it ideal to integrate with current Si BiCMOS technologies. Germanium will continue to become more integrated in Si processing as the ability to grow high-quality SiGe structures improves.

In this paper, we have presented the gain models for both homojunction and heterojunction bipolar phototransistors. It was found that even with a lower quality heterojunction interface, the HPT has superior current gain than the photo-BJT because of effective bandgap narrowing in the base region. For both devices, at a specified bit-error-rate, the given analysis could be extended to determine the SNR or number photons per bit for detection by a receiver system.

It is important to note that we have not considered frequency response in this analysis. Because of the importance of the gain-bandwidth product for integrated systems, the frequency characteristics of the bipolar phototransistor should also be designed for. In this case, the HBT has a speed advantage over the BJT because of the quasi-electric field created by the heterojunction. For the details of the frequency response, please refer to [15]. The transient response of these electrical devices could be easily applied to optical systems by replacing the voltage at the base-emitter electrode with a photo-voltage.

In conclusion, both the HPT and photo-BJT are optimized for operation in low SNR regimes because of their large current gain. Bipolar phototransistors detector schemes also offer low power consumption, and reduced circuit complexity and cost. The bipolar phototransistor is therefore a promising receiver for optical interconnects aimed at replacing traditional copper wiring.

Appendix A: Homojunction BJT Physics

In this section, we briefly review the physics of bipolar junction transistors (BJTs) [13]. Refer to the band diagram shown in Figure 2. Eventually, we will combine the mechanism of BJT gain with photoconductor theory to describe the response of a homo-junction bipolar phototransistor.

Consider an npn BJT with heavily-doped p-type region, lightly-doped n-type base, and p-type collector. We analyze the operation of the BJT in active mode as this is the region in which BJT amplifiers typically operate. The emitter-base junction (EBJ) is forward-biased and the collector-base junction (CBJ) is reverse-biased in active mode.

To derive the BJT gain parameter, we must obtain an expression for the base current in terms of the collector current i_C. The total base current i_B consists of two components:

(1) i_{B1}: electrons injected from the emitter to the base
(2) i_{B2}: holes supplied from the external bias voltage due to base recombination

We determine the first component of the base current by considering the electron diffusion from the emitter to the base. In the case of a thin base of width W, we can approximate the injected minority carrier electron concentration with a straight line profile:

$$n_p(x = 0) = n_{p0} e^{v_{BE}/V_T} \tag{A1}$$

$$n_p(x = W) = 0 \tag{A2}$$

The concentration goes to zero at $x = W$ because of the positively biased CBJ. Also, because the EBJ is a forward biased PN junction, this profile will be exponential with the emitter-base voltage v_{BE} and the thermal voltage V_T. We can now express the electron diffusion current in terms of the cross-section EBJ area A_E and electronic diffusivity D_n:

$$i_{B1} = A_E q D_n \frac{d}{dx} n_p(x) = \frac{A_E q D_n n_p(0)}{W} = \frac{A_E q D_n n_i^2}{N_A W} e^{v_{BE}/V_T} \tag{A3}$$

In the last line, I have used:

$$n_{p0} = \frac{n_i^2}{N_A} \tag{A4}$$

To derive the second component of the base current, we consider the charge Q_n injected into the base from the external bias. This base charge is the area under the triangular electron distribution given by equations (A1) and (A2):

$$Q_n = A_E \frac{q}{2} n_{p0} W = \frac{A_E q W n_i^2}{2N_A} e^{v_{BE}/V_T} \tag{A5}$$

Equation (A5) can be converted into a current by using the recombination lifetime τ_n of electrons in the base:

$$i_{B2} = \frac{A_E q W n_i^2}{2N_A \tau_n} e^{v_{BE}/V_T} \tag{A6}$$

At this point, we can define the base transport factor α_T, which quantifies the loss of carriers due to recombination in the base.

$$\alpha_T = \frac{i_{B1} - i_{B2}}{i_{B1}} = 1 - \frac{i_{B2}}{i_{B1}} = 1 - \frac{W^2}{2D_n \tau_n} = 1 - \frac{W^2}{2L_n^2} \tag{A7}$$

Now, before expressing the total base current, it is also useful to define the gain parameter:

$$\beta = \frac{1}{\frac{W^2}{2D_n \tau_n} + \frac{W D_p N_A}{L_p D_n N_D}} \tag{A8}$$

and the short circuit current I_s:

$$I_s = \frac{A_E q W n_i^2}{2N_A} \tag{A9}$$

Using the Einstein relation to put together these equations:

$$L_n = \sqrt{D_n \tau_n} \tag{A10}$$

we obtain an expression for the base current in terms of the collector current for a BJT:

$$i_B = i_{B1} + i_{B2} = \frac{I_s}{\beta} e^{v_{BE}/V_T} = \frac{i_C}{\beta} \tag{A11}$$

Equations (A8) and (A11) contain a great deal of information about the gain mechanism of a bipolar transistor. Some key observations:

(1) The base current depends exponentially on the base-emitter voltage.
(2) The gain parameter is approximately quadratic with the base width.
(3) The gain parameter can be increased by decreasing N_A/N_D (lightly doped base and heavily doped emitter).

These three observations will be re-visited in the context of photo-BJTs.

Appendix B: Photoconductors

In this section, we establish the amount of photo-induced charge on a doped semiconductor [14]. This approach will be combined with the gain of a bipolar transistor to determine the response of a photo-BJT.

To begin, consider a surface-illuminated p-type photoconducting material of width w and cross-sectional area ld. Assuming that each absorbed photon creates an electron-hole pair (EHP), the amount of charge in the material can be expressed as:

$$\delta n = \delta p \tag{B1}$$

$$n = n_0 + \delta n \tag{B2}$$

$$p = p_0 + \delta p \tag{B3}$$

where n_0 and p_0 are the electron and hole concentration, respectively, before light is shone on the material. For a p-type semiconductor ($p_0 \gg n_0$) with low-level injection ($p_0 \gg \delta p$), the rate equation is:

$$\frac{\partial}{\partial t}\delta n = G_0(t) - R_n = G_0(t) - \frac{\delta n}{\tau_n} \tag{B4}$$

where $G_0(t)$ and R_n are the generation and recombination rates, respectively, and τ_n is the electron recombination rate. We will consider the case of constant light:

$$\delta n = G_0 \tau_n \tag{B5}$$

In reality, the number of absorbed photons producing an electron-hole pair depends on the total quantum efficiency η. Thus, the net optical generation rate is the photon flux ($P_{opt}/h\upsilon$) per unit volume.

$$G_0 = \eta \frac{P_{opt}/h\upsilon}{lwd} \tag{B6}$$

The total quantum efficiency depends on the surface reflection coefficient R, the intrinsic material quantum efficiency η_i, and the absorption coefficient α. For a surface with an anti-reflection coating, we approximate $R = 1$. Therefore:

$$\eta = \eta_i(1 - e^{-\alpha d}) \tag{B7}$$

From equations (B5-B7), we note how the generation rate depends on the material quality and power of the incoming light. These two factors will be important when analyzing the bipolar transistor with a photo-conductive base.

Appendix C: Heterojunction BJT Physics

Now we consider the gain of a single heterojunction bipolar transistor (HBT) and compare it that of a homojunction BJT [15]. This physics will eventually be applied to a HPT. Refer to the HBT band diagram shown in Figure 5. The heterojunction is between the emitter and base while the collector and base are made of the same material.

We start by analyzing the electron concentrations with no voltage applied across the emitter base junction (EBJ). The majority-carrier electron concentration in the n-type emitter is:

$$N_{d,e} = n_{n0,e} = N_{c,e}\exp\left(-\frac{E_{c,e}-E_f}{kT}\right) \tag{C1}$$

The minority-carrier electron concentration in the p-type base is:

$$N_{a,b} = n_{p0,b} = N_{c,b}\exp\left(-\frac{E_{c,b}-E_f}{kT}\right) \tag{C2}$$

The conduction band energies $E_{c,e}$ and $E_{c,b}$ are related by the junction barrier heights for electrons and holes:

$$\phi_n = \frac{E_{c,e}-E_{c,b}}{q} \tag{C3}$$

$$\phi_p = \frac{E_{c,e}-E_{c,b}+\Delta E_g}{q} \tag{C4}$$

Under an applied bias v_{BE}, we can relate the majority carrier electron diffusion current $J_{n,b}$ from emitter to base. From PN junction theory, we know this current depends exponentially dependent on the applied voltage, diffusivity D_n, and diffusion length L_n.

$$J_{n,e} = -\frac{qD_n}{L_n}n_{p0,b}\left[e^{\frac{v_{BE}}{V_T}}-1\right] = -\frac{qD_n}{L_n}\frac{n_{i,b}^2}{N_{a,b}}\left[e^{\frac{v_{BE}}{V_T}}-1\right] \tag{C5}$$

We can write an analogous expression for the minority carrier hole diffusion current $J_{p,e}$.

$$J_{p,e} = -\frac{qD_p}{L_p}p_{n0,e}\left[e^{\frac{v_{BE}}{V_T}}-1\right] = -\frac{qD_p}{L_p}\frac{n_{i,e}^2}{N_{d,e}}\left[e^{\frac{v_{BE}}{V_T}}-1\right] \tag{C6}$$

But for the HBT, we want to express this current in terms of the carrier density in the emitter. Combining equations (C1-C4), we can re-write the electron diffusion current in terms of the intrinsic carrier density in the emitter.

$$J_{n,e} = -\frac{qD_n}{L_n}\frac{n_{i,e}^2}{N_{a,e}}\left[e^{\frac{v_{BE}}{V_T}} - 1\right]\exp\left(\frac{\Delta E_g}{kT}\right) \tag{C7}$$

The current across the heterojunction is increased because of the lower barrier height for electron injection due to the bandgap difference. We can relate the base currents for a homojunction BJT and an HBT with a heavily doped emitter.

$$\frac{i_{n,b\rightarrow hetero}}{i_{n,b\rightarrow homo}} = \exp\left(\frac{\Delta E_g}{kT}\right) \tag{C8}$$

At this point, a useful parameter to define is the emitter injection efficiency, which compares the percentage of current flowing from emitter to base with the current flowing from base to emitter. It is an important measure of the gain efficiency of an HBT or BJT.

$$\gamma = \frac{I_{n,e}}{I_{n,e}+I_{p,e}} = \frac{1}{1+\frac{I_{p,e}}{I_{n,e}}} \tag{C9}$$

$$\gamma_{homo} = \left(1 + \frac{D_p L_n N_{a,b}}{D_n L_p N_{d,e}}\right)^{-1} \tag{C10}$$

$$\gamma_{hetero} = \left(1 + \frac{D_p L_n N_{a,b}}{D_n L_p N_{d,e}}\exp\left(-\frac{\Delta E_g}{kT}\right)\right)^{-1} \tag{C11}$$

To derive the gain of an HBT, we must consider the loss of carriers due to recombination in the base. For a heterojunction interface with defects, base recombination could be quite large. As derived in Appendix A, the base transport factor for a BJT is:

$$\alpha_T = 1 - \frac{W^2}{2L_n^2} \tag{C12}$$

where W is the base width and L_n is the base recombination length for electrons. Taking into account, the emitter injection efficiency and base transport factor, we can define the collector current in terms of the emitter current.

$$I_c = -\gamma_{hetero}\alpha_{T,hetero}I_E = -\alpha_{F,hetero}I_E \tag{C13}$$

From Kirchoff's current law, we know

$$0 = I_B + I_C + I_E = I_B - \frac{I_C}{\alpha_{F,hetero}} + I_C \tag{C14}$$

Solving for the collector current of a heterojunction, we obtain:

$$I_c = \frac{\gamma_{hetero}\alpha_{T,hetero}}{1-\gamma_{hetero}\alpha_{T},hetero} = \beta I_B \tag{C15}$$

Therefore, for an exponential dependence on the heterojunction bandgap difference, the current gain of an HBT depends on the same parameters as a homojunction BJT.

References:

[1] D. A. B. Miller and H. M. Ozaktas, "Limit to the bit-rate capacity of electrical interconnects from the aspect ratio of the system architecture," Journal of Parallel and Distributed Computing **41**, pp. 42-52 (1997).

[2] C. Svensson, "Electrical interconnects revitalized," Manuscript, pp. 1-12 (1998).

[3] D. A. B. Miller, "Are optical transistors the next logical step?" Nature Photonics **4**, pp. 3-5 (2010).

[4] J. W. Shi and F. –M. Kuo, "High speed Si/Ge-based photodiodes for optical interconnect applications," Integrated Microsystems, pp. 509-519 (2009).

[5] M.-J. Lee, H.-S. Kang and W.-Y. Choi, "Equivalent circuit model for Si avalanche photodetectors fabricated in standard CMOS process," IEEE Electron Device Letters, **29**, pp. 1115–1117 (2008).

[6] A. K. Okyay, A. J. Pethe, D. Kuzum, S. Latif, D. A. B. Miller and K. C. Saraswat, "SiGe optoelectronic metal-oxide semiconductor field-effect transistor," Optics Letters **32**, pp. 2022-2024 (2007).

[7] C.T. DeRose et al., "Ultra compact 45 GHz CMOS compatible germanium waveguide photodiode with low dark current," Optics Express, Vol. **19** No. 25, pp. 24897–24904 (2011).

[8] X. Luo, "Transistor-based Ge/SOI photodetector for integrated silicon photonics" Ph.D thesis, UC Berkeley (2011).

[9] Ali K. Okyay et. al., "Silicon germanium CMOS optoelectronic switching device: bringing light to latch," IEEE Transactions on Electronic Devices, Vol. **54** No. 12, pp. 3252-3259 (2007).

[10] W. Shockley, M. Sparks and G. K. Teal, "p-n Junction Transistor," Physical Review **83**, pp. 151-162 (1951).

[11] J. N. Shive, "The properties of germanium phototransistors," Journal of the Optical Society of America **43**, pp. 239-244 (1953).

[12] H. Kroemer, "Theory of a wide-gap emitter for transistors," Proceedings of the IRE **45**, pp. 1535-1537 (1957).

[13] A. S. Sedra and K. C. Smith, *Microelectronic Circuits*, New York: Oxford University Press, 6th Edition (2010).

[14] S. L. Chuang, *Physics of Photonic Devices*, New Jersey: John Wiley and Sons, 2nd Edition (2009).

[15] R. S. Muller and T. I. Kamins, *Device Electronics for Integrated Circuits*, New York: John Wiley and Sons, 3rd Edition (2003).